Available online at www.sciencedirect.com
SCIENCE DIRECT
Toxicology Letters 165 (2006) 88–100
Toxicology Letters
www.elsevier.com/locate/toxlet

Direct and indirect effects of single walled carbon nanotubes on RAW 264.7 macrophages: Role of iron

V.E. Kagan [a,b,*], Y.Y. Tyurina [a,b], V.A. Tyurin [a,b], N.V. Konduru [a,b], A.I. Potapovich [a,b], A.N. Osipov [a,b], E.R. Kisin [c], D. Schwegler-Berry [c], R. Mercer [c], V. Castranova [c], A.A. Shvedova [c]

[a] *Center for Free Radical and Antioxidant Health, University of Pittsburgh, Pittsburgh, PA, United States*
[b] *Department of Environmental and Occupational Health, University of Pittsburgh, Pittsburgh, PA, United States*
[c] *Physiology/Pathology Research Branch, Health Effects Laboratory Division, NIOSH, Morgantown, WV, United States*

Received 20 September 2005; received in revised form 6 February 2006; accepted 6 February 2006
Available online 9 March 2006

Abstract

Single-walled carbon nanotubes (SWCNT), nano-cylinders with an extremely small diameter (1–2 nm) and high aspect ratio, have unique physico-chemical, electronic and mechanical properties and may exhibit unusual interactions with cells and tissues, thus necessitating studies of their toxicity and health effects. Manufactured SWCNT usually contain significant amounts of iron that may act as a catalyst of oxidative stress. Because macrophages are the primary responders to different particles that initiate and propagate inflammatory reactions and oxidative stress, we utilized two types of SWCNT: (1) iron-rich (non-purified) SWCNT (26 wt.% of iron) and (2) iron-stripped (purified) SWCNT (0.23 wt.% of iron) to study their interactions with RAW 264.7 macrophages. Ultrasonication resulted in predominantly well-dispersed and separated SWCNT strands as evidenced by scanning electron microscopy. Neither purified nor non-purified SWCNT were able to generate intracellular production of superoxide radicals or nitric oxide in RAW 264.7 macrophages as documented by flow-cytometry and fluorescence microscopy. SWCNT with different iron content displayed different redox activity in a cell-free model system as revealed by EPR-detectable formation of ascorbate radicals resulting from ascorbate oxidation. In the presence of zymosan-stimulated RAW 264.7 macrophages, non-purified iron-rich SWCNT were more effective in generating hydroxyl radicals (documented by EPR spin-trapping with 5,5-dimethyl-1-pyrroline-*N*-oxide, DMPO) than purified SWCNT. Similarly, EPR spin-trapping experiments in the presence of zymosan-stimulated RAW 264.7 macrophages showed that non-purified SWCNT more effectively converted superoxide radicals generated by xanthine oxidase/xanthine into hydroxyl radicals as compared to purified SWCNT. Iron-rich SWCNT caused significant loss of intracellular low molecular weight thiols (GSH) and accumulation of lipid hydroperoxides in both zymosan-and PMA-stimulated RAW 264.7 macrophages. Catalase was able to partially protect macrophages against SWCNT induced elevation of biomarkers of oxidative stress (enhancement of lipid peroxidation and GSH depletion). Thus, the presence of iron in SWCNT may be important in determining redox-dependent responses of macrophages.

Keywords: Single wall carbon nanotubes; Macrophages; Iron; Inflammatory response; Superoxide; Hydroxyl radical; Lipid peroxidation; GSH; Ascorbate

* Corresponding author at: Center for Free Radical and Antioxidant Health, Department of EOH, Bridgeside Point, 100 Technology Drive, Suite 350, Pittsburgh, PA 15219, United States. Tel.: +1 412 624 9479; fax: +1 412 624 9361.
E-mail address: vkagan@eoh.pitt.edu (V.E. Kagan).

0378-4274/$ – see front matter © 2006 Elsevier Ireland Ltd. All rights reserved.
doi:10.1016/j.toxlet.2006.02.001

1. Introduction

Nano-materials are at the leading edge of the rapidly developing field of nanotechnology. Their unique size-dependent properties make these materials superior and indispensable in many areas of human activity. As nano-materials and nano-devices are developed, awareness is growing that their unusual physico-chemical properties may lead to new dilemmas in decision making and managing potential environmental and health risks. While benefits of nano-technology are widely publicized, the discussion of the potential effects of their widespread use in consumer and industrial products are just beginning to emerge (Service, 2004). Among different types of nano-particles, single-walled carbon nanotubes (SWCNT) with their unique electronic and mechanical properties may also exhibit unique biological interactions, thus necessitating studies of their health effects. The extremely small size (~1 nm in diameter) renders their chemical and physical properties fundamentally different from larger particles of the same composition. Therefore, the biological and toxicological effects of SWCNT cannot be predicted by extrapolation of data collected in experiments with fine carbon particles. The most commonly used technology in the manufacturing of SWCNT is catalytic disproportionation of gaseous carbon molecules supported on catalytic metal (iron) particles (Bladh et al., 2000). Thus, unpurified SWCNT usually contain significant amounts (up to 40 wt.%) of iron (Morjan et al., 2002) that may act as a catalyst of oxidative stress (Halliwell and Getteridge, 1993). Since, metal-containing SWCNT are likely more toxic than metal-free nanoparticles, efforts have been made to remove this iron by acid treatment; such purified SWCNT contain <0.4 wt.% iron (Gorelik et al., 2000).

Macrophages are the primary responders to different particles that initiate and propagate inflammatory reactions (Ohtsuka et al., 1995; Mossman and Churg, 1998). Our previous work has demonstrated that inflammatory response to purified SWCNT included recruitment and activation of macrophages in the lung of exposed animals (Shvedova et al., 2005). Because NADPH oxidase-driven production of reactive oxygen species (ROS) (superoxide radicals, H_2O_2) in macrophages provides a redox environment in which transition metals can fully realize their pro-oxidant potential, a combination of macrophage response with catalytically-competent metal-containing SWCNT may synergistically enhance damage to cells and tissues. To study these important redox interactions in the current study, we used a macrophage cell culture model (RAW 264.7 murine macrophages) and characterized their ability to respond to standard iron-containing SWCNT with those produced by deliberately iron-stripped SWCNT. We assessed oxidative stress by measuring specific free radical intermediates by EPR spectroscopy, intracellular production of superoxide radicals and nitric oxide ($NO^{\bullet}$) by flow-cytometry, as well as lipid peroxidation and GSH content of macrophages.

2. Methods

2.1. SWCNT particles

SWCNT (CNI Inc., Houston, TX) produced by the high pressure CO (HiPco) disproportionation technique, employing CO in a continuous-flow gas-phase as the carbon feedstock and $Fe(CO)_5$ as the iron-containing catalyst precursor (non-purified SWCNT) (Bronikowski et al., 2001). Purified SWCNT were prepared by acid treatment to remove metal contaminates (Gorelik et al., 2000). Specific surface area was measured at −196 °C by nitrogen absorption–desorption technique (Brunauer Emmet Teller method, BET) using SA3100 Surface Area and Pore Size Analyzer, (Beckman Coulter Inc, Fullerton, CA) while diameter was measured by transmission electron microscopy (TEM). The mean diameters of purified/non-purified SWCNT were 1–4 nm. Surface areas of non-purified and purified SWCNT were 950 and 1040 m^2/g, respectively. Chemical analysis of total elemental carbon and metal (iron) in SWCNT was performed at the Chemical Exposure and Monitoring Branch (DART/NIOSH, Cincinnati, OH). Elemental carbon in SWCNT was assessed according to NIOSH Manual of Analytical Methods (NMAN) (Bronikowski et al., 2001), while metal content (iron) was analyzed using nitric acid dissolution and inductively coupled plasma-atomic emission spectrometry (ICP-AES) performed according to NMAM method 7300 for trace metals. Analysis performed by NMAN 5040 revealed that purified SWCNT comprised of 99.7 wt.% elemental carbon. For purity assessment of HiPco SWCNT, we used several standard analytical techniques including thermo gravimetric analysis with differential scanning colorimetry (TGA–DSC), thermo-programming oxidation (TPO), and Raman and near-infrared (NIR) spectroscopy (Birch, 2003; Arepalli et al., 2004; Dresselhaus et al., 2004). Comparative analytical data obtained by TGA–DSC, TPO, NIR and Raman spectroscopy revealed that more than 99% of carbon content in the SWCNT HiPco product was accountable in a carbon nanotube morphology.

2.2. EPR measurements of paramagnetic iron in SWCNT

Analyses were performed with a JEOL JES-RE1X EPR spectrometer (Kyoto, Japan) whereby the instrument settings were as follows: microwave power, 10 mW; modulation amplitude, 0.1 mT; time constant, 0.1 s; scan range 5000 G; center field 3350 G; receiver gain 50.

2.3. Scanning electron microscopy (SEM) of SWCNT

The SWCNT were diluted in double-distilled water and filtered with a 0.4 μm nucleopore filter. The filter was attached with double-stick carbon tape on an aluminum mount and sputter coated with gold/palladium. Images were collected on a JEOL 6400 scanning electron microscope.

2.4. Cell culture and exposure to particles

RAW 264.7 macrophages (from the ATCC) were grown in DMEM supplemented with 10% heat inactivated fetal bovine serum (FBS, Invitrogen, Carlsbad, CA), 100 units/ml penicillin and 100 μg/ml streptomycin in a humidified atmosphere (5% CO_2 plus 95% air) at 37 °C. Macrophages (0.3×10^6 cells/ml) were exposed to both non-purified SWCNT containing 26.0 wt.% of iron (0.12–0.5 mg/ml) or purified SWCNT containing 0.23 wt.% of iron (0.12–0.5 mg/ml) for 1–2 h at 37 °C. SWCNT were ultrasonicated using Cole–Palmer ultrasonic homogenizer (3 cycles × 30 s) prior to exposure. We used soluble and insoluble stimulators of macrophages activity PMA (1 μM) and zymosan (0.25 mg/ml), respectively. Concentration of both non-purified and purified SWCNT used for the study was expressed as total SWCNT materials.

2.5. Superoxide production

Intracellular production of superoxide was assessed using dihydroethidium (DHE, Molecular Probes, Eugene, OR) oxidation assay (Zhao et al., 2003). Macrophages (0.3×10^6/well) were pre-incubated with DHE (10 μM for 10 min at 37 °C). Then RAW 264.7 macrophages were stimulated by zymosan (0.25 mg/ml) or SWCNT (26.0 wt.% of iron) or purified SWCNT (0.23 wt.% of iron) for 30 min at 37 °C. Cells were analyzed using a FACScan flow cytometer (Becton-Dickinson, San Jose, CA) with monitoring of fluorescence (Ex.: 488 nm, Em.: 565–585 nm, channel FL2). Ten thousand events were collected and analyzed using the CellQuest software (Becton-Dickinson, San Jose, CA). For fluorescence microscopy, cells were washed three times with PBS, fixed with a solution of 2% formaldehyde in PBS. Thus treated cells were examined under a Nikon ECLIPSE TE 200 fluorescence microscope (Tokyo, Japan) equipped with a digital Hamamatsu charge-coupled device camera (C4742-95-12NBR) and analyzed using the MetaImaging Series™ software version 4.6 (Universal Imaging Corp., Downingtown, PA). Extracellular superoxide was measured in incubation medium by an SOD-inhibitable cytochrome *c* reduction assay as described (Pick and Mizel, 1981).

2.6. Nitric oxide production

Intracellular production of nitric oxide was assessed using and 4,5-diaminofluorescein diacetate (DAF-2DA, Calbiochem, San Diego, CA) oxidation assay (Jourd'heuil, 2002). Naïve macrophages (0.3×10^6/well) and macrophages stimulated by lipopolysaccharide (LPS, 0.1 μg/ml for 6 h at 37 °C) were pre-incubated with DAF-2DA (2 μM for 1 h at 37 °C). Then naïve and LPS-treated RAW 264.7 macrophages were stimulated by zymosan (0.25 mg/ml) or SWCNT (26.0 wt.% of iron) or purified SWCNT (0.23 wt.% of iron) for 2 h at 37 °C. Cells were analyzed using a FACScan flow cytometer (Becton-Dickinson, San Jose, CA) with monitoring of fluorescence (Ex.: 488 nm, Em.: 530 nm, channel FL1). Ten thousand events were collected and analyzed using the CellQuest software (Becton-Dickinson, San Jose, CA). For fluorescence microscopy, cells were washed three times with PBS, fixed with a solution of 2% formaldehyde in PBS. Thus treated cells were examined under a Nikon ECLIPSE TE 200 fluorescence microscope (Tokyo, Japan) equipped with a digital Hamamatsu charge-coupled device camera (C4742-95-12NBR) and analyzed using the MetaImaging Series™ software version 4.6 (Universal Imaging Corp., Downingtown, PA).

2.7. EPR measurements of free radical intermediates

Ascorbate (10 μM) and a spin-trapping agent, 5,5-dimethyl-1-pyrroline-*N*-oxide (DMPO, Sigma) (100 mM), were used for radical detection. All measurements were performed using a JEOL JES-RE1X EPR spectrometer (Kyoto, Japan). Instrument settings were as follows: microwave power, 20 mW; modulation amplitude, 0.1 mT; time constant, 1.3 s. To quantitate the ratio of superoxide and hydroxyl radicals in the superimposed EPR signals of their DMPO spin adducts, we applied the software program, EPRware, which allows to separate individual spectra of each of spin adducts and calculate its concentration. Calculation of spin adduct concentration was based on the evaluation of double integral of the EPR spectrum of spin adduct of interest and comparing it with a standard. Using this protocol, the concentrations of DMPO–OH spin adducts have been determined. The variations of the spin adduct EPR spectra intensity did not exceed 4–5%. EPR spectra from each sample were reproduced five times.

2.8. Fluorescence assay for low molecular weight thiols (GSH)

Low molecular weight thiols (predominantly GSH) in RAW 264.7 macrophages were determined using ThioGlo™-1, a maleimide reagent, which produces a highly fluorescent adduct upon its reaction with SH-groups (Shvedova et al., 2000). GSH content was estimated by an immediate fluorescence response registered upon addition of ThioGlo™-1 to the cell homogenate (0.3×10^6 cells). A spectrofluorophotometer RF-5301PC (Shimadzu, Kyoto, Japan) was employed for the assay of fluorescence using excitation at 388 nm and emission at 500 nm.

2.9. Determination of lipid hydroperoxides

Total lipids were extracted from cells using a Folch procedure (Folch et al., 1957). Lipid phosphorus was deter-

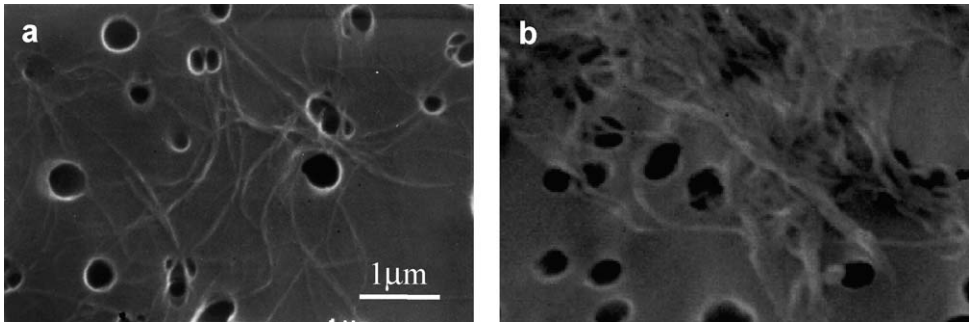

Fig. 1. SEM microphotographs of sonicated SWCNT on polycarbonate filter. SEM of purified SWCNT sample which was dispersed by ultrasonication and collected onto a 0.1 μm sized polycarbonate filter. (a) A view of separated strands. (b) A view of a poorly separated mat of the sample.

mined using micro-methods (Bottcher et al., 1961). Phospholipid hydroperoxides were determined by fluorescence HPLC of products formed in peroxidase-catalyzed reaction of fatty acid hydroperoxides (obtained by phospholipase A_2-catalyzed hydrolysis of specific oxidized phospholipids) with a fluorogenic substrate, Amplex Red, *N*-acetyl-3,7-dihydroxyphenoxazine (Kagan et al., 2005).

2.10. Statistics

The results are presented as mean ± S.D. values from at least three experiments, and statistical analyses were performed by either paired/unpaired Student's *t*-test or one-way ANOVA. The statistical significance of differences was set at $p < 0.05$.

3. Results

3.1. Characterization of iron levels in non-purifed and purified SWCNT

To study redox-catalytic role of iron in macrophage responses we utilized two types of SWCNT: (1) non-purified SWCNT obtained from CNI Corp. (Houston, TX), and (2) purified SWCNT obtained from NASA-JSC/SAIC, Advanced Technology Group (Houston, TX). To obtain more homogenous and dispersed suspension, SWCNT were ultrasonicated (30 s × 3 cycles). SEM microscopy of the samples showed that this sonication resulted in the production of a mixture containing predominantly well-dispersed and separated SWCNT strands (Fig. 1a) as well as small amounts of poorly separated mats of the sample (Fig. 1b). To characterize levels of iron, we employed ICP-AES analysis as well as EPR spectroscopy. ICP-AES analysis showed that iron levels were 260 mg Fe/g sample (26.0% by weight) and approximately 2.3 mg Fe/g sample (0.23 wt.%) in non-purified and purified SWCNT, respectively. Using EPR spectroscopy, we found that non-purified SWCNT displayed a broad signal with g value 2.0 and half-width of 64 mT attributable to high spin Fe^{3+} in a distorted tetrahedral environment (Fig. 2a) (Nozaki et al., 2002). The signal was hardly discernable in purified SWCNT (Fig. 2b).

In line with this different content of iron in the SWCNT samples, their redox-catalytic properties differed markedly. This was observed in the ability of SWCNT to catalyze one-electron oxidation of ascorbate to ascorbate radicals (Fig. 3a). While non-purified SWCNT samples induced appearance of a distinct and characteristic doublet signal of ascorbate radicals in EPR spectra (with hyperfine splitting constants of $a_H = 0.18$ mT) (Fig. 3b), purified SWCNT caused only

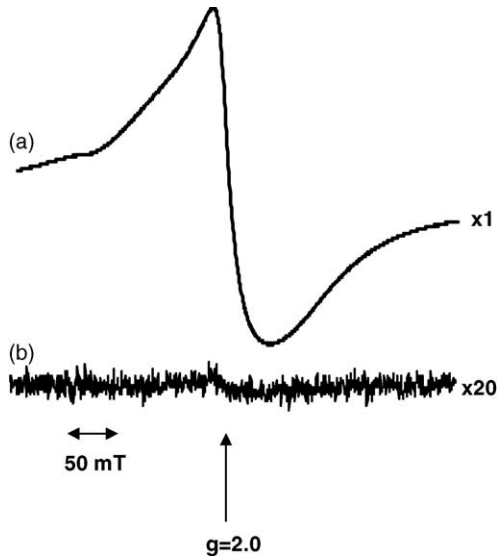

Fig. 2. EPR spectra of non-purified SWCNT and purified SWCNT. (a) Non-purified SWCNT (0.12 mg/ml, 26.0 wt.% of iron); (b) purified SWCNT (0.12 mg/ml, 0.23 wt.% of iron). Note that SWCNT displayed a broad signal with g value 2.0 and half-width of 64 mT attributable to high spin Fe^{3+} in a distorted tetrahedral environment; the signal was barely detectable in purified SWCNT sample.

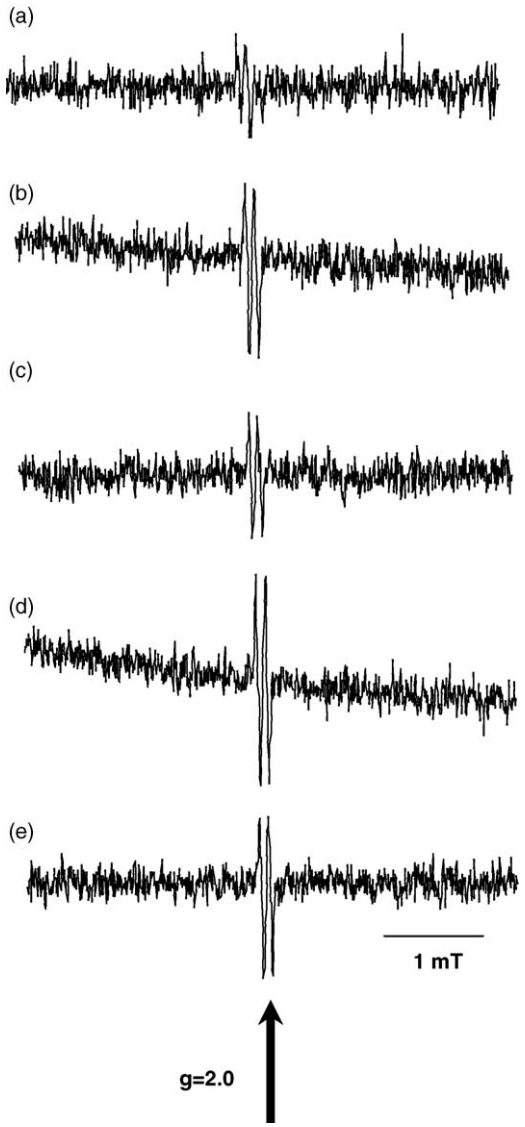

Fig. 3. EPR spectra of ascorbate radicals generated by non-purified and purified SWCNT in a cell-free system (a–c) and in the presence of zymosan-stimulated RAW 264.7 macrophages (d and e). Incubation system contained: ascorbate (10 μM) and non-purified SWCNT or (0.12 mg/ml, 26.0 wt.% of iron) or purified SWCNT (0.12 mg/ml, 0.23 wt.% of iron) in PBS (pH 7.4). EPR spectra (b–e) were recorded 5 min after addition of SWCNT. Zymosan (2.5 mg/ml)-stimulated RAW 264.7 macrophages (2×10^7 cells/ml) were present in experiments (d and e). (a) ascorbate; (b) acorbate plus non-purified SWCNT; (c) ascorbate plus purified SWCNT; (d) zymosan-stimulated RAW 264.7 macrophages plus non-purified SWCNT; (e) zymosan-stimulated RAW 264.7 macrophages plus purified SWCNT. Spectra "b" and "d" are tilted due to the overlap of the ascorbate radical signal with the iron signal present in non-purified SWCNT. EPR conditions: microwave power, 20 mW; modulation amplitude, 0.1 mT; time constant, 1.3 s; conversion time, 0.6 s. EPR measurements for each type of samples was reproduced at least five times and the differences between the samples usually did not exceed 4–5%.

a slight increase in the magnitude of the signal over its magnitude in the buffer (Fig. 3c).

3.2. Production of hydroxyl radicals by macrophages is enhanced by iron-containing SWCNT

We were anxious to find out whether this elevated redox activity of non-purified SCWNT could be realized in the presence of macrophages. It is possible, that superoxide radicals generated by activated macrophages during the oxidative burst can interact with iron-containing SWCNT via Fenton-chemistry reaction pathways. Therefore, we estimated the production and conversions of radicals by co-incubations of zymozan-activated RAW 264.7 macrophages with non-purified and purified SWCNT. In the first series of experiments, we used a spin trap, DMPO, to study radical generation by zymosan-stimulated macrophages (Fig. 4a). An enhanced generation of hydroxyl radical DMPO adducts (DMPO–OH) (with $a_N = 1.49$ mT, $a_H = 1.49$ mT) was detected when zymosan-stimulated RAW 264.7 macrophages were co-incubated with iron-containing non-purified SWCNT (compare Fig. 4b and Fig. 4a). A $15 \pm 4\%$ weaker EPR signal of hydroxyl radical DMPO adducts was observed in the presence of purified SWCNT. Thus, non-purified SWCNT are more effective in generating highly reactive oxidizing (hydroxyl) radicals in the presence of activated RAW 264.7 macrophages (Fig. 4c). Non-activated macrophages did not respond by radical production to co-incubations with either non-purified or purified SWCNT (Fig. 4d–f).

While intracellular production of ROS was not induced by SWCNT in RAW 264.7 macrophages, both intracellularly and extracellularly generated superoxide radicals can dismutate to H_2O_2; the latter can diffuse out of cells and undergo further reduction to reactive hydroxyl radicals, particularly in the presence of electron-rich iron-containing SWCNT (Forman and Torres, 2002). DMPO adducts of hydroxyl radicals [DMPO–OH] are more stable and more readily detectable in the presence of cells than DMPO superoxide radical adducts [DMPO–OOH]. The lack of detectable superoxide radical DMPO adducts by activated RAW 264.7 macrophages (Fig. 4a) may be due to a relatively low steady-state concentrations of superoxide radicals. To verify this, we decided to generate superoxide radicals by an enzymatic system xanthine/xanthine oxidase in the presence of RAW 264.7 macrophages. Using a spin trap, DMPO, we were able to clearly detect formation of two types of spin adducts: superoxide-

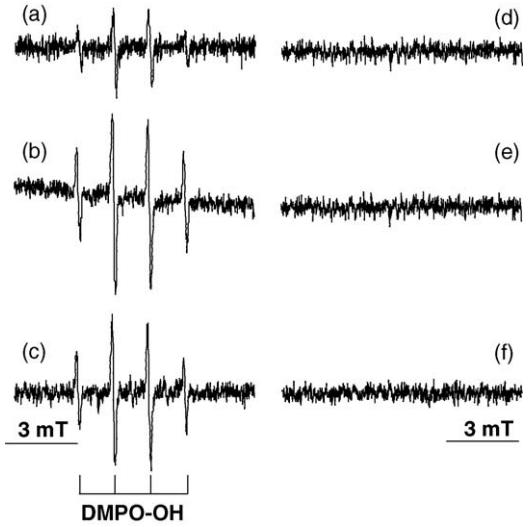

Fig. 4. EPR spectra of DMPO radical adducts generated during incubation of zymosan-stimulated or naïve RAW 264.7 macrophages in the presence and in the absence of SWCNT. Incubation system contained: zymosan (2.5 mg/ml)-stimulated or naïve RAW 264.7 macrophages (2×10^7 cells/ml), DMPO (100 mM), non-purified SWCNT (0.12 mg/ml, 26.0 wt.% of iron) or purified SWCNT (0.12 mg/ml, 0.23 wt.% of iron) in PBS (pH 7.4). Cells were incubated with SWCNT and DMPO for 30 min and EPR spectra were recorded. EPR conditions: microwave power, 20 mW; modulation amplitude, 0.1 mT; time constant, 1.3 s. (a) zymosan-stimulated RAW 264.7 macrophages plus DMPO; (b) zymosan-stimulated RAW 264.7 macrophages plus DMPO, plus non-purified SWCNT; (c) zymosan-stimulated RAW 264.7 macrophages plus DMPO, plus purified SWCNT; (d) naïve RAW 264.7 macrophages plus DMPO; (e) naïve RAW 264.7 macrophages plus DMPO, plus non-purified SWCNT; (f) naïve RAW 264.7 macrophages plus DMPO, plus purified SWCNT. Spectrum "b" is tilted due to the overlap of the spin adduct signal with the iron signal present in non-purified SWCNT. EPR measurements for each type of samples was reproduced at least five times and the differences between the samples usually did not exceed 4–5%.

DMPO adducts (with $a_N = 1.4$ mT, $a_H^\beta = 1.13$ mT, $a_H^\gamma = 0.16$ mT) ($79 \pm 4\%$ of the signal) and hydroxyl radical adducts ($21 \pm 3\%$ of the signal) (Fig. 5a). When non-purified SWCNT were added to the incubation system, a remarkably efficient conversion of superoxide radical adducts into hydroxyl radical adducts occurred such that the former now represented only $18 \pm 4\%$ of the signal whereas the latter were accountable for $82 \pm 5\%$ of the signal (Fig. 5b). A markedly less effective conversion of superoxide radical adducts into hydroxyl radical adducts was induced by purified SWCNT resulting in their contribution of $35 \pm 3\%$ and $65 \pm 5\%$ into the overall EPR signal, respectively (Fig. 5c).

We were able to detect weak EPR signals of DMPO–OH adducts from RAW 264.7 macrophages stimulated with PMA (data not shown). However, the

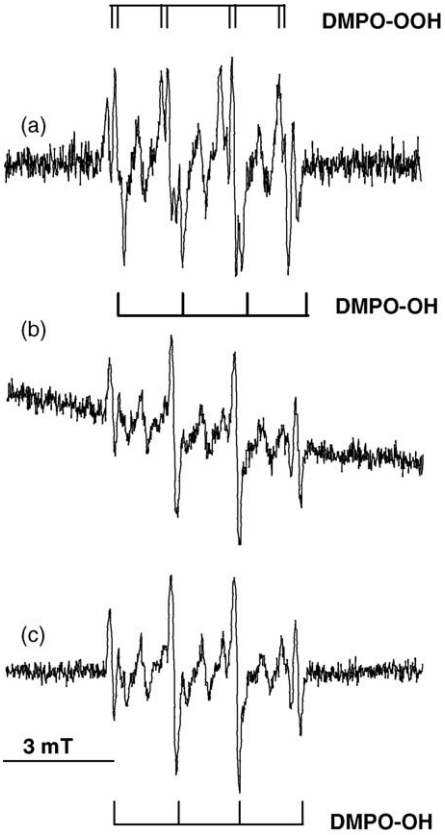

Fig. 5. EPR spectra of DMPO radical adducts generated during incubation of xanthine oxidase/xanthine and zymosan-stimulated RAW 264.7 macrophages in the presence and in the absence of SWCNT. Incubation system contained: xanthine oxidase (0.1 U/ml), xanthine (1 mM), zymosan (2.5 mg/ml)—stimulated RAW 264.7 macrophages (2×10^7 cells/ml), DMPO (100 mM); non-purified SWCNT (0.12 mg/ml, 26.0 wt.% of iron) or purified SWCNT (0.12 mg/ml, 0.4 wt.% of iron), PBS (pH 7.4). EPR spectra (b and c) were recorded 1 min after addition of SWCNT. EPR conditions: microwave power, 20 mW; modulation amplitude, 0.1 mT; time constant, 1.3 s. (a) zymosan-stimulated RAW 264.7 macrophages plus xanthine oxidase/xanthine, plus DMPO; (b) zymosan-stimulated RAW 264.7 macrophages plus xanthine oxidase/xanthine, plus DMPO, plus non-purified SWCNT; (c) zymosan-stimulated RAW 264.7 macrophages plus xanthine oxidase/xanthine, plus DMPO, plus purified SWCNT. Spectrum "b" is tilted due to the overlap of the spin adduct signal with the iron signal present in non-purified SWCNT. The variations of the spin adduct EPR spectra intensity did not exceed 4–5%. EPR spectra from each sample were reproduced five times. Note that typical EPR signals of superoxide-DMPO adducts markedly decreased, whereas spin adducts of hydroxyl radicals increased upon addition of purified SWCNT.

EPR signal of DMPO–OH adducts was significantly less pronounced than that generated in zymosan-stimulated macrophages. This was due to a rapid oxidation of the spin trap and the adduct, most likely by PMA-induced peroxidase activity in macrophages. Indeed,

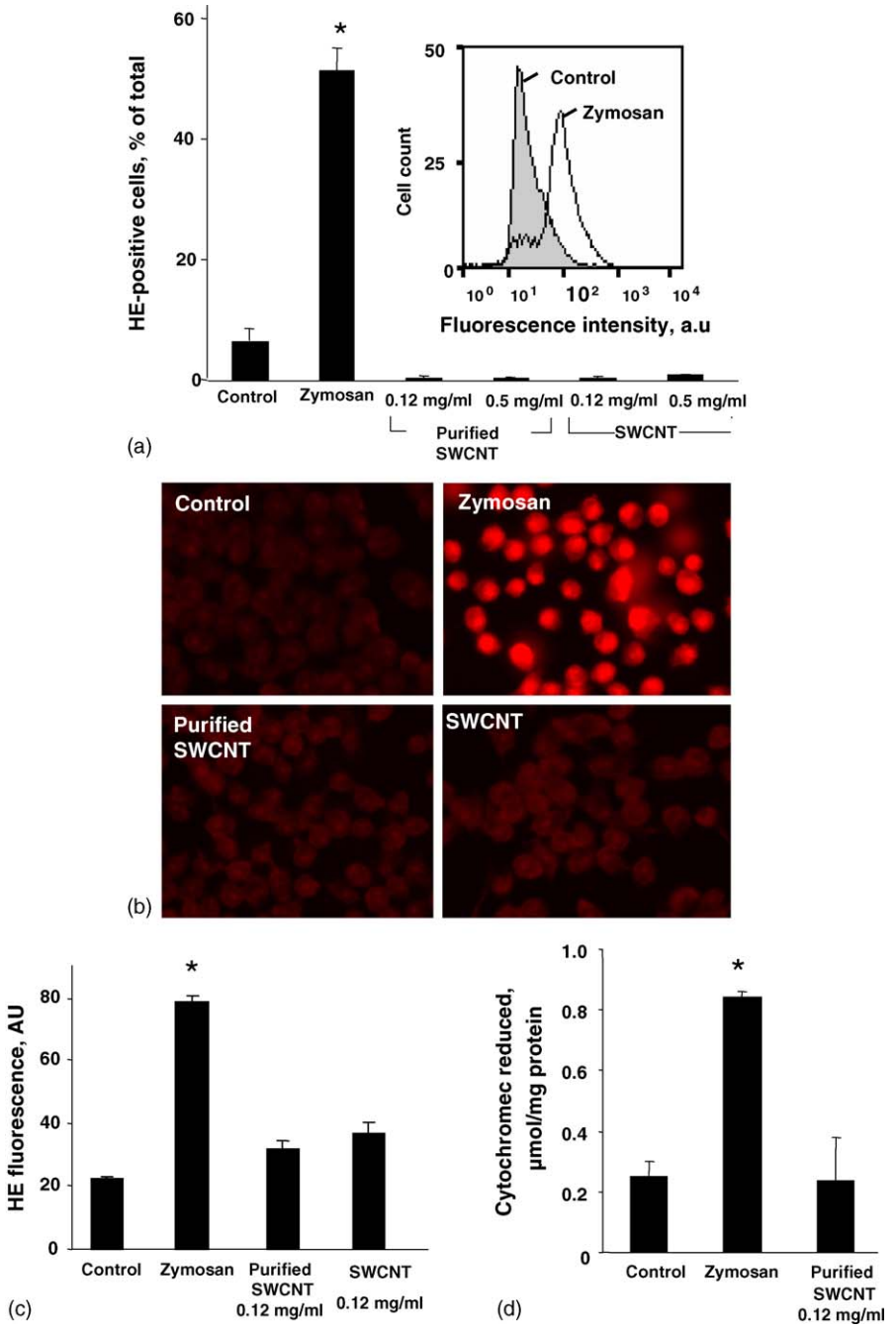

Fig. 6. Production of superoxide in RAW 264.7 macrophages after stimulation by zymosan or SWCNT. (a) Production of superoxide in RAW 264.7 macrophages after stimulation by zymosan or SWCNT as evidenced by flow-cytometry with DHE. *Insert*: typical histograms showing distribution of cells with hydroxyethydium (HE) fluorescence response from non-treated and zymosan-treated RAW 264.7 macrophages. Macrophages (0.3×10^6 cells/well) were pre-incubated with DHE (10 μM) for 10 min at 37 °C. Then RAW 264.7 macrophages were stimulated by zymosan or either non-purified SWCNT (0.12 mg/ml, 26.0 wt.% of iron) or purified SWCNT (0.12 mg/ml, 0.23 wt.% of iron) for 30 min at 37 °C. Data are means ± S.D., $n = 8$; $^*p < 0.05$ vs. control cells. (b) Evaluation of the number of superoxide producing cells by fluorescence microscopy of DHE oxidation. Photomicrographs are representative of three independent experiments. (c) Fluorescence intensity obtained from the superoxide producing RAW 264.7 macrophages. Data are means ± S.D.; $n = 5$; $^*p < 0.05$ vs. control cells. (d) Reduction of cytochrome *c* by RAW 264.7 macrophages stimulated with zymosan (0.25 mg/ml) or purified SWCNT (0.12 mg/ml). Macrophages (0.3×10^6 cells/well) were stimulated by zymosan or either non-purified SWCNT (0.12 mg/ml, 26.0 wt.% of iron) or purified SWCNT (0.12 mg/ml, 0.23 wt.% of iron) for 30 min at 37 °C in the presence of cytochrome *c* (100 μM). Data are means ± S.D.; $n = 3$; $^*p < 0.05$ vs. control cells.

stimulation of macrophages with PMA has been shown to result in significant activation of myeloperoxidase (MPO) (Rodrigues et al., 2002). Furthermore, high MPO activity has been reported to limit the applications of EPR spin-trapping for the detection of hydroxyl radical spin-adducts (Britigan et al., 1986; Cohen et al., 1988). Additionally, macrophages with activated MPO produce a highly reactive radical species, $ClO^{\bullet}{}_2$ (Rodrigues et al., 2002) readily converting DMPO and DMPO–OH adducts into nitroxides (Ozawa et al., 1996). In line with this, we observed the appearance of a triplet signal in the EPR spectra obtained from PMA-stimulated macrophages.

3.3. Intracellular oxidative/nitrosative stress in SWCNT-treated RAW 264.7 macrophages

Our previous work established that macrophages did not effectively engulf and phagocytoze non-functionalized purified SWCNT and did not respond by intracellular production of reactive oxygen and nitrogen species to stimulation with purified SWCNT (Shvedova et al., 2005). Therefore, we were eager to determine the extent to which non-purified SWCNT with enhanced capacity to catalyze oxidative/nitrosative stress are active in stimulating intracellular production of superoxide radicals and $NO^{\bullet}$ by RAW 264.7 macrophages. We incubated RAW 264.7 macrophages with non-purified and purified SWCNT and studied their ability to intracellularly generate superoxide radicals and $NO^{\bullet}$ by flow-cytometry using DHE and DAF-2DA as specific probes, respectively (Jourd'heuil, 2002; Zhao et al., 2003). Flow-cytometry measurements using DHE showed that neither non-purified nor purified SWCNT at two different concentrations (0.12 and 0.5 mg/ml) were able to stimulate the production of superoxide radicals by RAW 264.7 macrophages (Fig. 6a). In contrast, zymosan, a prototypical activator of macrophages (Ezekowitz and Gordon, 1986) caused a robust intracellular production of superoxide and increased the number of DHE-positive cells from $6.7 \pm 1.6\%$ in control to $50.8 \pm 3.3\%$ after the exposure (Fig. 6a). In addition, we performed experiments in which we used two independent assessments of superoxide production. The number of superoxide producing cells was evaluated by fluorescence microscopy of DHE oxidation. Extracellular generation of superoxide radicals was determined by a SOD-inhibitable cytochrome *c* reduction assay. Using DHE, we found that neither non-purified nor purified SWCNT (0.12 mg/ml) were able to stimulate intracellular production of superoxide radicals in RAW 264.7 macrophages as was evidenced by fluorescence microscopy (Fig. 6b and c). Similarly, SWCNT were not effective in activating oxidative burst (superoxide production) assessed by cytochrome *c* reduction (Fig. 6d).

Similarly, generation of $NO^{\bullet}$ in DAF-2DA-loaded RAW 264.7 macrophages revealed no response to both types of SWCNT (0.12 and 0.5 mg/ml) although a significantly increased number of DAF-2-positive cells was observed after stimulation of cells with LPS (plus zymosan) as was evidenced by flow-cytometry (Fig. 7a) and fluorescence microscopy (Fig. 7b). Thus SWCNT were not effective in activating oxidative (superoxide production) or nitrosative (nitric oxide production) stress in RAW 264.7 macrophages independently on the absence or presence of iron in the particles.

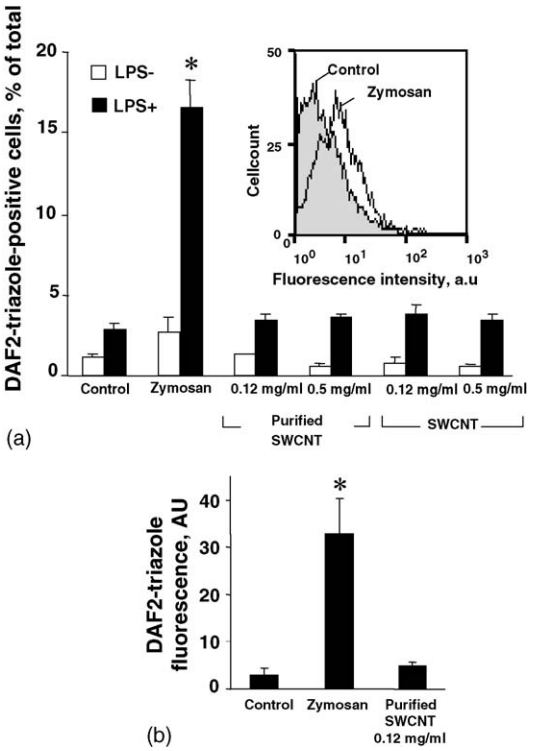

Fig. 7. Production of NO in RAW 264.7 macrophages after stimulation by zymosan or SWCNT. (a) Production of NO in RAW 264.7 macrophages after stimulation by zymosan or SWCNT as evidenced by flow-cytometry with DAF-2. Naïve macrophages (0.3×10^6/well) and macrophages stimulated by LPS (0.1 μg/ml for 6 h at 37 °C) were pre-incubated with DAF-2DA (2 μM for 1 h at 37 °C). Then RAW 264.7 macrophages were stimulated by zymosan or non-purified SWCNT (0.12 mg/ml, 26.0 wt.% of iron) or purified SWCNT (0.12 mg/ml, 0.23 wt.% of iron) for 2 h at 37 °C. Data are means ± S.D.; $n = 8$; $^{*}p < 0.05$ vs. control cells. *Insert*: typical histograms showing distribution of cells with DAF-2 triazole fluorescence response from non-treated and zymosan-treated RAW 264.7 macrophages. (b) Fluorescence intensity obtained from the NO producing RAW 264.7 macrophages. Data are means ± S.D., $n = 5$; $^{*}p < 0.05$ vs. control cells.

3.4. Macrophages as targets of SWCNT-enhanced oxidative stress

While intracellular production of ROS was not induced by SWCNT in RAW 264.7 macrophages, extracellularly generated superoxide radicals can dismutate to H_2O_2 and act as a source of highly oxidizing (hydroxyl) radicals, particularly in the presence of iron-rich SWCNT. Thus, oxidative burst generated by activated macrophages can be enhanced by SWCNT and cause oxidative stress via extracellular oxidative pathways. Additionally, H_2O_2 can diffuse into cells where it can be activated to act as a potent oxidant. To test the hypothesis, we assessed whether changes in the content of major antioxidants, ascorbate and GSH, and an important and specific biomarker of oxidative stress, phospholipid hydroperoxides, could be detected in RAW 264.7 macrophages challenged with non-purified SWCNT.

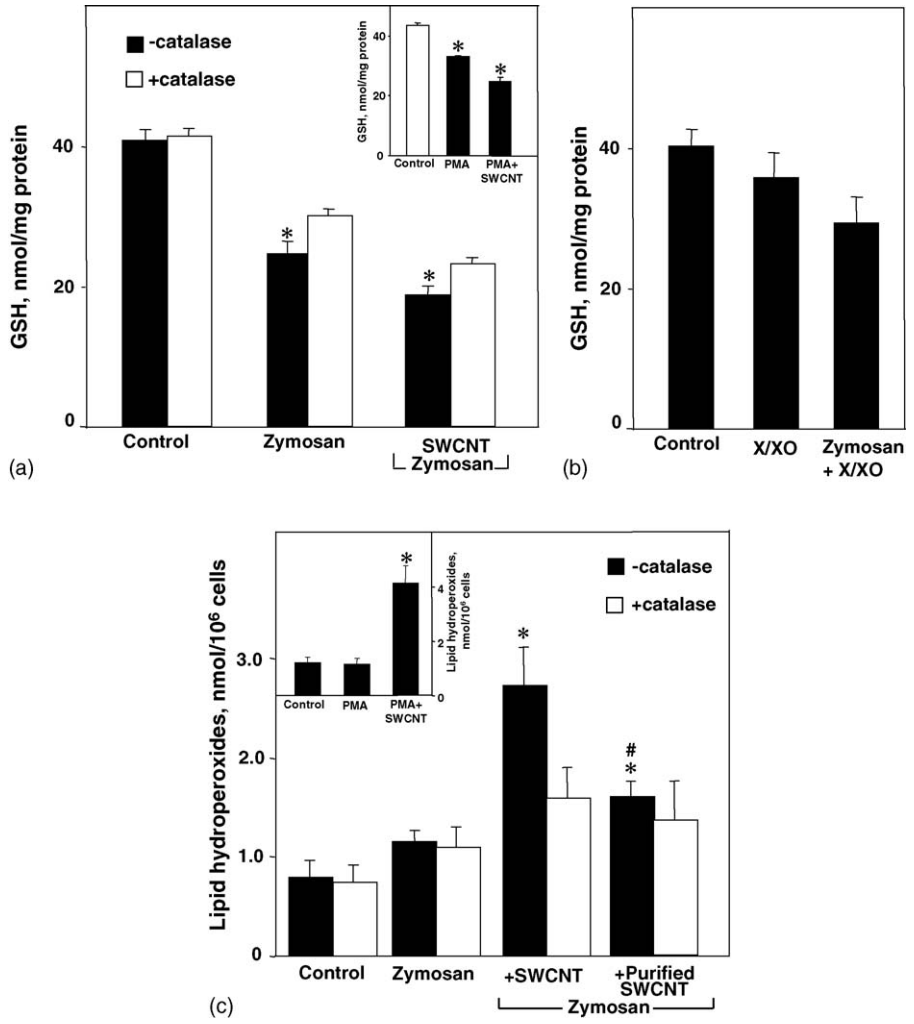

Fig. 8. Effect of SWCNT exposure on GSH content and lipid peroxidation in RAW 264.7 macrophages. (a) GSH content in zymosan- and PMA (*inset*) stimulated RAW 264.7 macrophages exposed to SWCNT. Zymosan (0.25 mg/ml)- or PMA (1 μM)-stimulated RAW 264.7 macrophages (0.3×10^6 cells/well) were incubated in the presence of non-purified (0.12 mg/ml, 26.0 wt.% of iron) or purified (0.12 mg/ml, 0.23 wt.% of iron) SWCNT for 2 h and 30 min at 37 °C, respectively. To remove extracellular H_2O_2 in some experiments catalase (75 U/ml) was added prior to any additions. (b) Effect of xantine/xantine oxidase on GSH content in normal and zymosan-stimulated RAW 264.7 macrophages. Control (0.3×10^6 cells/well) or zymosan-stimulated (0.3×10^6 cells/well) cells were treated with xantine (1 mM) and xantine oxidase (0.1 U/ml) for 30 min at 37 °C. (c) Accumulation of lipid hydroperoxides in zymosan- and PMA (*inset*) stimulated RAW 264.7 macrophages exposed to SWCNT. Zymosan (0.25 mg/ml)- or PMA (1 μM)-stimulated RAW 264.7 macrophages (0.3×10^6 cells/well) were incubated in the presence of non-purified (0.12 mg/ml, 26.0 wt.% of iron) or purified (0.12 mg/ml, 0.23 wt.% of iron) SWCNT for 2 h and 30 min at 37 °C, respectively. To remove extracellular H_2O_2 in some experiments catalase (75 U/ml) was added prior to any additions. Data are means ± S.D.; $n = 5$; $^{*}p < 0.05$ vs. control cells. $^{\#}p < 0.05$ vs. non-purified SWCNT.

Indeed, in the presence of ascorbate, zymosan-activated macrophages responded to non-purified SWCNT by a strong production of ascorbate radicals, one-electron oxidation products of ascorbate (Fig. 3d). This response was iron-dependent as a markedly weaker EPR signal of ascorbate radicals was detectable in the presence of purified SWCNT (Fig. 3e). Further, incubation of zymosan-stimulated RAW 264.7 macrophages with non-purified SWCNT for 2 h caused a two-fold decrease of the GSH content in macrophages (Fig. 8a). Similarly, in PMA-stimulated RAW 264.7 macrophages SWCNT caused a two-fold decrease of the GSH content (Fig. 8a, inset). Finally, low levels of lipid hydroperoxides in control cells (0.8 nmol/10^6 cells) were increased by zymosan stimulation. A low endogenous level of lipid hydroperoxides in macrophages was increased by SWCNT in PMA-stimulated macrophages (Fig. 8c, inset)—in line with our results with zymosan-stimulated macrophages (Fig. 8b).

While iron can interact with H_2O_2, the production of hydroxyl radical requires an addition of one electron usually donated by the reduced ferrous form of iron. As a result, the presence of superoxide may be essential in that it maintains iron in its reduced form ready to act as an electron donor. Diffusion of H_2O_2 and its extracellular scavenging by catalase is entirely possible. Therefore, we performed assessments of the effects of catalase on SWCNT induced changes of GSH and lipid hydroperoxides levels. We found that catalase was able to partially protect from SWCNT induced: (1) decrease of GSH (Fig. 8a) and (2) accumulation of lipid hydroperoxides (Fig. 8c). In line with these results, our additional experiments with extracellularly produced superoxide (using xanthine/xanthine oxidase system) demonstrated a depletion of GSH in RAW 264.7 macrophages (Fig. 8b). This suggests that dismutation of superoxide to H_2O_2 and subsequent diffusion of the latter into cells may be responsible, at least in part, for the oxidative stress occurring in macrophages during inflammatory response. Thus iron-containing SWCNT are capable of enhancing oxidative stress in zymosan-activated macrophages.

4. Discussion

One of the most commonly used technologies in the manufacturing of SWCNT is catalytic disproportionation of gaseous carbon molecules supported on catalytic iron particles (high-pressure CO conversion, HiPco^{TM}). In this process ($CO + CO \xrightarrow{Fe} C + CO_2$), the decorating (encapsulated) iron particles were found to have cross sections between 2 and 10 nm and constitute up to 40 wt.% of iron in crude SWCNT (Morjan et al., 2002). Several attempts have been made to reduce/remove iron from the final product. One of the best techniques allows purification of gram-scale quantities of SWCNT using a modification of a gas-phase purification technique previously reported by Chiang et al. (Chiang et al., 2001) with high-temperature oxidations and repeated extractions with nitric and hydrochloric acid. This improved procedure significantly reduces the amount of impurities within the SWCNT and increases their stability. As a result, the iron content of the SWCNT can be dramatically reduced but still remained at the level of 0.2 wt.%. This suggests that toxicological assessments of SWCNT exposures should take into consideration significant presence of catalytically active iron in SWCNT.

Potentially high pulmonary toxicity of SWCNT (compared to quartz particles, an ultrafine carbon black particles) has been reported (Huzcko et al., 1997; Elder et al., 2004; Lam et al., 2004; Rao et al., 2004; Warheit et al., 2004). However, the presence, importance, and cytotoxic mechanisms of SWCNT iron, to the best of our knowledge, have not been addressed. Our recent findings indicate that iron-enriched SWCNT had a significantly more pronounced toxic effect on cultured cells (keratinocytes, broncho-alveolar epithelial cells) than SWCNT treated with iron chelators (Shvedova et al., 2003a,b, 2005).

Particle-induced inflammation is believed to include activation of macrophages (oxidative burst, generation and release of pro-inflammatory mediators) and phagocytosis of particles. This initial inflammatory reaction is followed by phagocytosis of apoptotically dying cells and production and release of anti-inflammatory and profibrogenic mediators that initiate the deposition of collagen (Junqueira et al., 1979). Our previously published results indicate that, contrary to this well established chain of events, non-functionalized SWCNT are not particularly well recognized by macrophages, hence are not active as targets of macrophage engulfment and phagocytosis (Shvedova et al., 2005). Similarly, the results of the present study demonstrate that neither iron-rich (non-purified) nor purified SWCNT were able to induce intracellular production of superoxide or nitric oxide by RAW 264.7 macrophages. Consequently, the failure of macrophages to recognize dispersed SWCNT in vivo may result in their diffusion into systemic circulation, dissemination, and subsequent effects on distant tissues including cardiovascular damage and brain injury. These distant effects of nanoparticles, including SWCNT have been reported (Oberdorster et al., 2004; Li et al., 2005; Oberdorster et al., 2005).

We showed that iron content of SWCNT was important for enhanced catalysis of extracellular oxidative stress as well as for intracellular depletion of antioxidant reserves (ascorbate, GSH) and accumulation of lipid peroxidation products in macrophages. This enhancement of oxidative stress by iron-containing SWCNT can change the normal course of macrophage-dependent development of the inflammatory response. In particular, an abbreviated production of pro-inflammatory cytokines and very early switch to the generation of pro-fibrogenic anti-inflammatory cytokines, accompanied by very early deposition of collagen and elastin was detected in C57BL/6J mice after aspiration of SWCNT (Shvedova et al., 2005). Redox environment of macrophages is known to substantially affect their pro-/anti-inflammatory responses (Forman and Torres, 2001). It is possible that iron-dependent changes of redox status of macrophages as well as of their extracellular milieu is capable of altering their activation and cytokine profiles from acute pro-inflammatory to pro-fibrogenic. In fact, SWCNT caused more robust production and release of anti-inflammatory pro-fibrogenic cytokines such as TGF-β and IL-10 (as compared to pro-inflammatory cytokines TNF-α and IL-1β) from RAW 264.7 macrophages in vitro (Shvedova et al., 2005).

Macrophages function as 'pathogen sensors' and are essential for the elimination of pathogens as well as for the regulation of the adaptive immune response and the inflammatory response (Plowden et al., 2004). These critical functions of macrophages depend on a number of different markers and receptors on their surface, among which toll-like receptors (TLR) play a very important role. Commonly, activation of macrophages includes TLR-mediated stimulation of NADPH-oxidase and NO-synthase (NOS) via different signaling pathways (Karupiah et al., 2000). TLR-2-dependent mechanisms are mainly engaged in NADPH-oxidase activation, whereas NOS activation is induced through TLR-4 signaling (Kleeberger et al., 2001; Frost et al., 2004). The enhanced intracellular production of ROS and NO, required for effective phagocytosis and digestion of bacteria by macrophages (Forman and Torres, 2001; Torres and Forman, 2003), is usually associated with subsequent triggering of their apoptotic death (DeLeo, 2004). We were unable to detect activation of these ROS- and NO-generating signaling pathways by either iron-rich (non-purified) or iron-stripped (purified) SWCNT. Not surprisingly, no SWCNT induced enhancement of apoptosis was observed (Shvedova et al., 2005).

If indeed macrophage failure to recognize dispersed SWCNT is essential for the unusual time course of pulmonary inflammatory response to SWCNT and early onset of fibrogenesis, one may think about strategies to stimulate the recognition and engulfment of SWCNT by macrophages via modifying the SWCNT surface by appropriate ligands. One interesting strategy may be based on the utilization of phosphatidylserine receptor-mediated pathway. In fact our preliminary experiments indicate that phosphatidylserine adsorbed on the surface made SWCNT recognizable by RAW 264.7 macrophages. In line with this, a recent report indicated that modification of SWCNT surface by a detergent, Pluronic, also resulted in their effective recognition by macrophages in vitro (Cherukuri et al., 2004). It is worth mentioning, however, that TLR-mediated activation of NADPH-oxidase and NO-synthase in macrophages are regulated by both phosphatidylserine signaling and oxidative stress (Serinkan et al., 2005). Further studies are necessary to more specifically characterize the mechanisms and pathways through which enhanced oxidative stress and phosphatidylserine signaling by apoptotic cells change pro- and anti-inflammatory profiles of macrophage responses, hence affect the time course of inflammation and fibrosis in SWCNT exposed animals.

5. Disclaimers

The finding and conclusions in this report are those of the authors and do not necessary represent the view of the National Institute for Occupational Safety and Health.

Acknowledgements

This work was supported by NIOSH grant 1RO1 OH-008282, NIH 1RO1 HL-070755, NORA 6927007Y and NORA 6927Z1LU.

References

Arepalli, S., Nikolaev, P., Gorelik, O., 2004. Analytical characterization of single wall carbon nanotubes. Encyclopedia Nanosci. Nanotechnol. 1, 51–66.

Birch, M.E., 2003. Elemental carbon. Monitoring of diesel exhaust particulate in the workplace. NIOSH Manual of Analytical Methods (NMAM 5040), vol. chapter Q., 4th ed. DHHS publication, NIOSH, Cincinnati, OH, p. 2154.

Bladh, K., Falk, L.K.L., Rohmund, F., 2000. On the iron-catalyzed growth of single-walled carbon nanotubes and encapsulated metal particles in the gas phase. Appl. Phys. A 70, 317–322.

Bottcher, C.J.F., van Gent, C.M., Pries, C., 1961. A rapid and sensitive sub-micro phosphorus determination. Anal. Chim. Acta 24, 2003–2004.

Britigan, B.E., Rosen, G.M., Thompson, B.Y., Chai, Y., Cohen, M.S., 1986. Stimulated human neutrophils limit iron-catalyzed hydroxyl radical formation as detected by spin-trapping techniques. J. Biol. Chem. 261, 17026–17032.

Bronikowski, M.J., Willis, P., Colbert, D.T., Smith, K.A., Smalley, R.E., 1800. Gas-phase production of carbon single-walled nanotubes from carbon monoxide via the HiPco process: a parametric study. J. Vac. Sci. Technol. 19.

Cherukuri, P., Bachilo, S.M., Litovsky, S.H., Weisman, R.B., 2004. Near-infrared fluorescence microscopy of single-walled carbon nanotubes in phagocytic cells. J. Am. Chem. Soc. 126, 15638–15639.

Chiang, I.W., Brinson, B.E., Huang, A.Y., Willis, P.A., Bronikowski, M.J., Margrave, J.L., Smalley, R.E., Hauge, R.H., 2001. Purification and characterization of single-wall carbon nanotubes (SWNTs) obtained from the gas-phase decomposition of CO (HiPco Process). J. Phys. Chem. B. 105, 8297–8301.

Cohen, M.S., Britigan, B.E., Hassett, D.J., Rosen, G.M., 1988. Do humans neutrophils form hydroxyl radical? Evaluation of an unresolved controversy. Free Radical Biol. Med. 5, 81–88.

DeLeo, F.R., 2004. Modulation of phagocyte apoptosis by bacterial pathogens. Apoptosis 9, 399–413.

Dresselhaus, M.S., Dresselhaus, G., Charlier, J.C., Hernandez, E., 2004. Electronic, thermal and mechanical properties of carbon nanotube. Philos. Trans. Ser. A Math. Phys. Eng. Sci. 362, 2065–2098.

Elder, A.C., Gelein, R., Azadniv, M., Frampton, M., Finkelstein, J., Oberdorster, G., 2004. Systemic effects of inhaled ultrafine particles in two compromised, aged rat strains. Inhal. Toxicol. 16, 461–471.

Ezekowitz, R.A., Gordon, S., 1986. Interaction and regulation of macrophage receptors. Ciba Found. Symp. 118, 127–136.

Folch, J., Lees, M., Sloan-Stanley, G.H., 1957. A simple method for isolation and purification of total lipids from animal tissue. J. Biol. Chem. 226, 497–509.

Forman, H.J., Torres, M., 2001. Redox signaling in macrophages. Mol. Aspects Med. 22, 189–216.

Forman, H.J., Torres, M., 2002. Reactive oxygen species and cell signaling: respiratory burst in macrophage signaling. Am. J. Respir. Crit. Care Med. 166, S4–S8.

Frost, R.A., Nystrom, G.J., Lang, C.H., 2004. Lipopolysaccharide stimulates nitric oxide synthase-2 expression in murine skeletal muscle and C(2)C(12) myoblasts via toll-like receptor-4 and c-Jun NH(2)-terminal kinase pathways. Am. J. Physiol. Cell Physiol. 287, C1605–C1615.

Gorelik, O., Nikolaev, P., Arepalli, S., 2000. Purification procedures for single-wall carbon nanotubes, NASA contractor report, NASA/CR-2000-208926.

Halliwell, B., Getteridge, J.M.C., 1993. Free radicals in biology and medicine. Clarendon Press, Oxford.

Huzcko, A., Lange, H., Calko, E., Grubek-Jaworska, H., Droszcz, P., 1997. Physiological testing of carbon nanotubes: are they asbestos-like? Fullerene Sci. Technol. 9, 251–254.

Jourd'heuil, D., 2002. Increased nitric oxide-dependent nitrosalation of 4,5-diaminofluorescein by oxidants: implication for the measurement of intracellular nitric oxide. Free Radical Biol. Med. 33, 676–684.

Junqueira, L.C., Bignolas, G., Brentani, R.R., 1979. Picrosirius staining plus polarization microscopy, a specific method for collagen detection in tissue sections. Histochem. J. 11, 447–455.

Kagan, V.E., Tyurin, V.A., Jiang, J., Tyurina, Y.Y., Ritov, V.B., Amoscato, A.A., Osipov, A.N., Belikova, N.A., Kapralov, A.A., Kini, V., Vlasova, I.I., Zhao, Q., Zou, M., Di, P., Svistunenko, D.A., Kurnikov, I.V., Borisenko, G.G., 2005. cytochrome *c* acts as a cardiolipin oxygenase required for release of pro-apoptotic factors. Nat. Chem. Biol. 1, 223–232.

Karupiah, G., Hunt, N.H., King, N.J., Chaudhri, G., 2000. NADPH oxidase, Nramp1 and nitric oxide synthase 2 in the host antimicrobial response. Rev. Immunogenet. 2, 387–415.

Kleeberger, S.R., Reddy, S.P., Zhang, L.Y., Cho, H.Y., Jedlicka, A.E., 2001. Toll-like receptor 4 mediates ozone-induced murine lung hyperpermeability via inducible nitric oxide synthase. Am. J. Physiol. Lung Cell Mol. Physiol. 280, L326–L333.

Lam, C.W., James, J.T., McCluskey, R., Hunter, R.L., 2004. Pulmonary toxicity of single-wall carbon nanotubes in mice 7 and 90 days after intratracheal instillation. Toxicol Sci. 77, 126–134.

Li, V., Salmen, R., Huldermen, T., Kisin, E.R., Shvedova, A.A., Luster, M.I., Simeonova, P.P., 2005. Pulmonary exposure to carbon nanotubes induces vascular toxicity. Toxicologist 84, 213.

Morjan, R.E., Nerushev, O.A., Sveningsson, M., Falk, L.K.L., Rohmund, F., Campbell, E.E.B., 2002. Parametric study of nanotube growth from C2H2 and C60 on supported iron catalyst particles. AIP Conf. Proc. 633, 186.

Mossman, B.T., Churg, A., 1998. Mechanisms in the pathogenesis of asbestosis and silicosis. Am. J. Respir. Crit. Care Med. 157, 1666–1680.

Nozaki, C., Lugmair, C.G., Bell, A.T., Tilley, T.D., 2002. Synthesis, characterization, and catalytic performance of single-site iron(III) centers on the surface of SBA-15 silica. J. Am. Chem. Soc. 124, 3194–13203.

Oberdorster, G., Oberdorster, E., Oberdorster, J., 2005. Nanotoxicology: an emerging discipline evolving from studies of ultrafine particles. Environ. Health Perspect. 113, 823–839.

Oberdorster, G., Sharp, Z., Atudorei, V., Elder, A., Gelein, R., Kreyling, W., Cox, C., 2004. Translocation of inhaled ultrafine particles to the brain. Inhal. Toxicol. 16, 437–445.

Ohtsuka, Y., Munakata, M., Ukita, H., Takahashi, T., Satoh, A., Homma, Y., Kawakami, Y., 1995. Increased susceptibility to silicosis and TNF-alpha production in C57BL/6J mice. Am. J. Respir. Crit. Care Med. 152, 2144–2149.

Ozawa, T., Miura, Y., Ueda, J., 1996. Oxidation of spin-traps by chlorine dioxide (ClO_2) radical in aqueous solutions: first ESR evidence of formation of new nitroxide radicals. Free Radical Biol. Med. 20, 837–841.

Pick, E., Mizel, D., 1981. Rapid microassays for the measurement of superoxide and hydrohen peroxide production by macrophages in culture using an automatic enzyme immunoassay reader. J. Immunol. Methods 46, 211–226.

Plowden, J., Renshaw-Hoelscher, M., Engleman, C., Katz, J., Sambhara, S., 2004. Innate immunity in aging: impact on macrophage function. Aging Cell 3, 161–167.

Rao, K.M., Porter, D.W., Meighan, T., Castranova, V., 2004. The sources of inflammatory mediators in the lung after silica exposure. Environ. Health Perspect. 112, 1679–1686.

Rodrigues, M.R., Rodriguez, D., Russo, M., Campa, A., 2002. Macrophage activation includes high intracellular myeloperoxidase activity. Biochem. Biophys. Res. Commun. 292, 869–873.

Serinkan, B.F., Gambelli, F., Potapovich, A.I., Babu, H., Di Giuseppe, M., Ortiz, L.A., Fabisiak, J.P., Kagan, V.E., 2005. Apoptotic cells quench reactive oxygen and nitrogen species and modulate TNF-alpha/TGF-beta 1 balance in activated macrophages: involvement of phosphatidylserine-dependent and- independent pathways. Cell Death Differ. 12, 1141–1144.

Service, R.F., 2004. Nanotoxicology. Nanotechnology grows up. Science 304, 1732–1734.

Shvedova, A.A., Castranova, V., Kisin, E.R., Schwegler-Berry, D., Murray, A.R., Gandelsman, V.Z., Maynard, A., Baron, P., 2003a. Exposure to carbon nanotube material: assessment of nanotube

cytotoxicity using human keratinocyte cells. J. Toxicol. Environ. Health A. 66, 1909–1926.

Shvedova, A.A., Kisin, E.R., Mercer, R., Murray, A.R., Johnson, V.J., Potapovich, A.I., Tyurina, Y.Y., Gorelik, O., Arepalli, S., Schwegler-Berry, D., Hubbs, A.F., Antonini, J., Evans, D.E., Ku, B.K., Ramsey, D., Maynard, A., Kagan, V.E., Castranova, V., Baron, P., 2005. Unusual inflammatory and fibrogenic pulmonary responses to single walled carbon nanotubes in mice. Am. J. Physiol. Lung Cell Mol. Physiol. 289, L698–L708.

Shvedova, A.A., Kommineni, C., Jeffries, B.A., Castranova, V., Tyurina, Y.Y., Tyurin, V.A., Serbinova, E.A., Fabisiak, J.P., Kagan, V.E., 2000. Redox cycling of phenol induces oxidative stress in human epidermal keratinocytes. J. Invest. Dermatol. 114, 354–364.

Shvedova, A.A., Murray, A.R., Kisin, E.R., Schwegler-Berry, D., Kagan, V.E., Gandelsman, V.Z., Castranova, V., 2003b. Exposure to carbon nanotube material: evidence of exposure-induced oxidant stress in human keratinocyte and bronchial epithelial cells. Free Radical Res. 37, 97.

Torres, M., Forman, H.J., 2003. Redox signaling and the MAP kinase pathways. Biofactors 17, 287–296.

Warheit, D.B., Laurence, B.R., Reed, K.L., Roach, D.H., Reynolds, G.A., Webb, T.R., 2004. Comparative pulmonary toxicity assessment of single wall carbon nanotubes in rats. Toxicol. Sci. 77, 117–125.

Zhao, H., Kalivendi, S., Zhang, H., Joseph, J., Nithipatikom, K., Vasquez-Vivar, J., Kalyanaraman, B., 2003. Superoxide reacts with hydroethidine but forms a fluorescenct product that is distinctly different from ethidium: potential implications in intracellular fluorescence detection of superoxide. Free Radical Biol. Med. 34, 1359–1368.